Discovery of a dual-action small molecule that improves neuropathological features of Alzheimer's disease mice

Min Hee Park[a,b,1], Kang Ho Park[a,b,1], Byung Jo Choi[a,c], Wan Hui Han[a,b], Hee Ji Yoon[a,b], Hye Yoon Jung[a,b], Jihoon Lee[d], Im-Sook Song[d], Dong Yu Lim[e], Min-Koo Choi[e], Yang-Ha Lee[f], Cheol-Min Park[f], Ming Wang[g], Jihoon Jo[h,i], Hee-Jin Kim[j], Seung Hyun Kim[j], Edward H. Schuchman[k], Hee Kyung Jin[a,c,2], and Jae-sung Bae[a,b,2]

[a]KNU Alzheimer's Disease Research Institute, Kyungpook National University, Daegu 41566, South Korea; [b]Department of Physiology, Cell and Matrix Research Institute, School of Medicine, Kyungpook National University, Daegu 41944, South Korea; [c]Department of Laboratory Animal Medicine, College of Veterinary Medicine, Kyungpook National University, Daegu 41566, South Korea; [d]BK21 FOUR Community-Based Intelligent Novel Drug Discovery Education Unit, Vessel-Organ Interaction Research Center (VOICE), College of Pharmacy and Research Institute of Pharmaceutical Sciences, Kyungpook National University, Daegu 41566, South Korea; [e]College of Pharmacy, Dankook University, Cheon-an 31116, South Korea; [f]Department of Chemistry, Ulsan National Institute of Science and Technology, Ulsan 44919, South Korea; [g]BioMedical Sciences Graduate Program, Chonnam National University, Hwasun 58128, South Korea; [h]Department of Biomedical Sciences, Chonnam National University Medical School, Gwangju 501-757, South Korea; [i]Department of Neurology, Chonnam National University Medical School, Gwangju 501-757, South Korea; [j]Department of Neurology, Hanyang University College of Medicine, Seoul 04763, South Korea; and [k]Department of Genetics and Genomic Sciences, Icahn School of Medicine at Mount Sinai, New York, NY 10029

Edited by Hugo Bellen, Department of Molecular and Human Genetics and Department of Neuroscience, Baylor College of Medicine, Houston, TX; received August 16, 2021; accepted November 15, 2021

Alzheimer's disease (AD) is characterized by complex, multifactorial neuropathology, suggesting that small molecules targeting multiple neuropathological factors are likely required to successfully impact clinical progression. Acid sphingomyelinase (ASM) activation has been recognized as an important contributor to these neuropathological features in AD, leading to the concept of using ASM inhibitors for the treatment of this disorder. Here we report the identification of KARI 201, a direct ASM inhibitor evaluated for AD treatment. KARI 201 exhibits highly selective inhibition effects on ASM, with excellent pharmacokinetic properties, especially with regard to brain distribution. Unexpectedly, we found another role of KARI 201 as a ghrelin receptor agonist, which also has therapeutic potential for AD treatment. This dual role of KARI 201 in neurons efficiently rescued neuropathological features in AD mice, including amyloid beta deposition, autophagy dysfunction, neuroinflammation, synaptic loss, and decreased hippocampal neurogenesis and synaptic plasticity, leading to an improvement in memory function. Our data highlight the possibility of potential clinical application of KARI 201 as an innovative and multifaceted drug for AD treatment.

Alzheimer's disease | ASM direct inhibitor | GHSR1 alpha agonist | memory improvement | small compound

Alzheimer's disease (AD) is a multifaceted neurodegenerative disease with underlying pathologies that extend well beyond the widely recognized accumulation of amyloid beta (Aβ). Many studies have demonstrated that memory impairment in AD is driven by the interaction of various pathologic processes, such as cell death (1), impaired synapse plasticity (2), neurogenesis loss (3), autophagy dysfunction (4), vascular abnormalities (5), blood–brain barrier (BBB) damage (6), and systemic inflammation (7). Thus, effective drug development for this disorder must focus on therapeutic strategies that target the complex and multiple neuropathological features in AD.

We and others have previously reported that the activity of several sphingolipid-metabolizing enzymes, especially acid sphingomyelinase (ASM), which is encoded by the *SMPD1* gene, is abnormally expressed in AD patients and mouse models (8–10). The primary role of ASM is to catalyze the conversion of sphingomyelin, a major component of membranes, into ceramide and phosphocholine (11). The increased ASM activity in the blood and brain of AD mice contributes to various pathological features, including cell apoptosis (12), defective autophagy (8), neurogenesis loss (13), BBB leakage (14), and inflammation (15, 16), suggesting that ASM inhibition could be an important therapeutic target that addresses the neuropathological features of AD (17). Although some studies have previously identified direct or indirect functional inhibitors (17–20) of ASM, these inhibitors have lacked specificity, leading to the potential for off-target effects and unclear potential mechanisms of action in AD. Therefore, there is an important need to develop new compounds that block ASM activity by direct interaction with the enzyme.

Here, we identify KARI 201 as a direct, selective, and competitive ASM inhibitor with excellent brain distribution and druggability. Interestingly, we also found an unexpected role of

Significance

Since Alzheimer's disease (AD) is a multifaceted neurodegenerative disease, multitargeted therapeutic approaches are likely required for effective AD treatment. The importance of acid sphingomyelinase (ASM) activation in the various neuropathological features of AD is well-known. Therefore, in this study, we focused on identifying an efficient, direct inhibitor of ASM activity. We found that KARI 201 was a highly selective ASM activity inhibitor without any off-target effects. Through RNA-sequencing analysis in brains of AD mice, we also unexpectedly uncovered the role of KARI 201 as a ghrelin receptor agonist. This dual role of KARI 201 in neurons led to improvement of Aβ accumulation, neuroinflammation, synapse loss, hippocampal neurogenesis, and memory dysfunction in AD mice.

Author contributions: M.H.P., K.H.P., H.K.J., and J.-s.B. designed research; M.H.P., K.H.P., B.J.C., W.H.H., H.J.Y., H.Y.J., J.L., I.-S.S., D.Y.L., M.-K.C., M.W., and J.J. performed research; Y.-H.L. and C.-M.P. contributed new reagents/analytic tools; H.-J.K. and S.H.K. performed normal and AD patient plasma experiments; E.H.S., H.K.J., and J.-s.B. interpreted data; B.J.C., W.H.H., H.J.Y., H.Y.J., J.L., I.-S.S., D.Y.L., M.-K.C., M.W., J.J., H.-J.K., and S.H.K. analyzed data; and M.H.P., K.H.P., E.H.S., H.K.J., and J.-s.B. wrote the paper.

The authors declare no competing interest.

This article is a PNAS Direct Submission.

[1]M.H.P. and K.H.P. contributed equally to this work.

[2]To whom correspondence may be addressed. Email: hkjin@knu.ac.kr or jsbae@knu.ac.kr.

This article contains supporting information online at http://www.pnas.org/lookup/suppl/doi:10.1073/pnas.2115082119/-/DCSupplemental.

Published January 13, 2022.

KARI 201 as an agonist of growth hormone secretagogue receptor 1α (GHSR1α, also known as the ghrelin receptor) via GPCR (G protein–coupled receptor) screening based on RNA-sequencing (RNA-seq) analysis in KARI 201–treated AD mice. This activity is critical for hippocampal synaptic physiology and may impact neuropathological features in AD as well (21–23). The dual action in neurons of KARI 201 as a direct ASM inhibitor and GHSR1α agonist led to outstanding, synergetic therapeutic effects in AD mouse models on neuropathological features involving learning and memory impairment. Therefore, our data highlight the possibility of clinical application of KARI 201 as an innovative and multifaceted drug for AD treatment.

Results

ASM Activity Increases with AD Progression and KARI Compounds Directly Inhibit ASM Activity. Based on previous reports (8–10), we further investigated ASM activity in the plasma of AD patients with disease progression (*SI Appendix*, Table S1). The data showed that ASM activity in plasma increased as the disease progressed, again suggesting the importance of ASM as a target to reduce neuropathological features in AD (*SI Appendix*, Fig. S1).

Screening through cell-based ASM activity assays was performed using a total of 1,273 chemical compounds obtained from the Korea Chemical Bank (functional inhibitors of ASM [FIASMA] derivative-targeted library) and Ulsan National Institute of Science and Technology (sphingolipid-targeted library). The screening was carried out in AD patient fibroblasts (*presenilin 1*, PS1-familial AD) with an abundant ASM activity (8) at a chemical concentration of 10 μM. This led to discovery of the 2-amino-2-(1,2,3-triazol-4-yl)propane-1,3-diol (KARI) series of inhibitors. Biochemical potency optimization of the KARI backbone was performed by the addition of alkyl groups of varying chain lengths to enhance lipophilicity and BBB permeability (24, 25). This optimization led to the identification of KARI 501 (6-carbon chain), KARI 401 (7-carbon chain), KARI 301 (8-carbon chain), KARI 201 (9-carbon chain), and KARI 101 (10-carbon chain). Further assays were performed to assess the best compound with regard to direct ASM inhibition, druggability, and therapeutic efficacy for AD, and KARI 201 was finally chosen as shown in *SI Appendix*, Fig. S2.

First, ASM binding affinity was evaluated in biosensor experiments using surface plasmon resonance (SPR) detection. Sensorgrams for each compound showed dose-dependent binding to ASM. KARI 501, 301, 201, and 101 exhibited high binding affinity (K_D) according to the number of carbons in the alkyl chain; KARI 401 showed lower binding affinity than the other compounds (*SI Appendix*, Fig. S3*A*). We also observed high ASM inhibitory potency by KARI compounds depending on carbon chain length (*SI Appendix*, Fig. S3*B*). Thus, these results indicated that compounds containing alkyl groups with longer carbon chains had higher ASM binding and direct inhibitory effects, suggesting that the length of alkyl group played an important role in stable ASM binding.

Next, the cellular activity of the KARI compounds was evaluated in AD patient fibroblasts compared with amitriptyline (AMI), which is a commonly used functional inhibitor of ASM (19). After 30 min of treatment with the KARI compounds or AMI, ASM activity detected in cell lysates was efficiently inhibited. Particularly, KARI 201 and 101 showed higher inhibition effects than AMI (*SI Appendix*, Fig. S4*A*). Although no significant differences in sphingomyelin content were observed between the groups, ceramide production was decreased by KARI compounds or AMI (*SI Appendix*, Fig. S4 *B* and *C*).

To investigate other potential mechanisms of ASM activity inhibition, we followed *SMPD1* messenger RNA (mRNA) and ASM protein expression levels. *SMPD1* mRNA was not downregulated and ASM protein levels were also not significantly changed by KARI compounds (*SI Appendix*, Fig. S4 *D* and *E*), indicating that KARI compounds inhibited ASM activity without changing mRNA and protein levels. We further confirmed the direct inhibition effects of the KARI compounds on the secretory form of ASM using PS1-derived supernatant medium (P-sup). For these studies the assay buffer contained zinc to activate the enzyme, as previously described (19). KARI compounds, especially KARI 201 and 101, exhibited a more significant inhibition effect on secretory ASM than others. In contrast, AMI did not inhibit ASM activity in this setting (*SI Appendix*, Fig. S4*F*). These results showed that KARI compounds directly inhibited both lysosomal and secretory ASM activity in AD patient cells.

AMI has been reported to induce the proteolytic degradation of ASM in lysosomes, and this effect was prevented by pretreatment with the serine/cysteine protease inhibitor leupeptin (26). Preincubation with leupeptin prevented ASM inhibition induced by AMI, confirming these findings, but not by the KARI compounds (*SI Appendix*, Fig. S4*G*). Consistent with previous results (19), AMI treatment also altered lysosomal pH, detected by the acidotropic dye LysoTracker red, and induced accumulation of phospholipids labeled by LipidTOX reagent, while KARI compounds had no significant effect on the mean fluorescence intensity (MFI) of either LysoTracker or LipidTOX (*SI Appendix*, Fig. S4 *H* and *I*). These results suggested that KARI compounds could directly inhibit ASM activity without an effect on the lysosomal compartment. KARI compounds also did not cause cell death and alteration of other sphingolipid metabolic enzymes, sphingolipids, and sphingolipid-related receptor levels (*SI Appendix*, Figs. S4 *J* and *K* and S5), indicating the selective effect of KARI compounds on ASM activity inhibition.

Next, based on the results of the binding affinity, IC_{50}, and in vitro efficacy, we selected KARI 201 and KARI 101 as highly potent direct inhibitors of ASM activity for further analysis. KARI 501 also was selected to help assess the importance of the number of carbons in the chains. The results of cell-based IC_{50} against ASM activity and ceramide production using the three compounds showed a carbon chain–dependent inhibitory effect (*SI Appendix*, Fig. S6), again demonstrating the critical role of carbon chain length in efficient inhibition of ASM activity.

KARI 201 Is a Selective and Competitive Inhibitor of ASM with Excellent Pharmacokinetic Properties. Before investigating the ASM inhibition effects of KARI compounds in an AD mouse model, we examined the pharmacokinetic (PK) properties of three compounds (KARI 501, 201, and 101). First, the single-dose PK profiles and brain distributions of the three compounds were assessed. We observed that compounds with longer carbon chains showed lower systemic bioavailability, while distribution into the brain was higher (*SI Appendix*, Fig. S7 *A* and *B*). At 24 h post administration, KARI 201 or KARI 101 showed the highest concentrations in the brain, while KARI 501 exhibited similar distribution tendencies between tissues (*SI Appendix*, Fig. S7*C*). In metabolic stability assays using human and liver microsomes, KARI 501 and 201 exhibited high stability, while KARI 101 showed weak stability (*SI Appendix*, Fig. S8*A*). These results suggested that the long carbon chain of KARI 101 might be unstable in vivo, even though this compound exhibited the best ability to cross the BBB. These data of drug–drug interaction potential of these compounds revealed that KARI 201 was the best compound with no effects on inhibition of the seven major cytochrome P450 enzymes

(*SI Appendix*, Fig. S8*B*). Therefore, KARI 201 was finally selected for further study based on its excellent PK properties.

Next, to assess the effects of KARI 201 (10 μM) on other enzyme activities, the kinase activities of 430 kinases and 38 additional enzymes were tested. Results exhibiting kinase activity lower than 30% or other enzyme inhibition higher than 50% were considered to represent significant effects of KARI 201. However, we observed no substantial off-target effects of this compound in these functional panels (*SI Appendix*, Fig. S9), highlighting that KARI 201 is a selective ASM inhibitor.

We also carried out molecular docking calculations in order to better understand the mechanism of ASM inhibition by KARI 201. The active site in ASM defines a stringent specificity for two zinc ions, which are coordinated by catalytic residues containing four histidines, two aspartic acids, and one asparagine (27–29). Recent studies presented the crystal structure of ASM, with detailed information on how the two zinc ions and sphingomyelin and/or the product phosphocholine are coordinated by the enzyme (27–29). Based on the crystal structure of ASM, we began by building a model of KARI 201 bound to ASM. Docking simulations revealed that KARI 201 occupied an active-site domain of ASM, which was also the sphingomyelin and/or phosphocholine binding site (27–29) (Fig. 1*A*). Detailed analysis also suggested that one of hydroxyl groups of KARI 201 resided within a zinc binding site. Histidine 282 (H282), H319, and H457 are catalytic residues of ASM that interact with the amino group, triazole group, and hydroxyl group of KARI 201, respectively (Fig. 1 *B* and *C*). These binding interactions based on our model were consistent with those in the crystal structure of the ASM–phosphocholine complex, suggesting that KARI 201 might be compatible with the phosphocholine-binding pocket of ASM (Fig. 1*D*).

Based on these data, we further investigated whether KARI 201 inhibited sphingomyelin binding to the ASM active site. Incorporation of KARI 201 into ASM was decreased with increasing concentrations of sphingomyelin, yielding K_M values of 332.5, 433.9, and 572.6 μM at 1, 10, and 100 μM KARI 201, respectively (Fig. 1*E*). These data demonstrated that KARI 201 exhibited a competitive mode of inhibition versus sphingomyelin. Collectively, our results strongly suggested that KARI 201 is a selective and competitive inhibitor of ASM with excellent PK properties for therapeutic application in AD and potentially other disorders.

KARI 201 Improves Neuropathological Features in APP/PS1 Mice. To determine the inhibition effects of ASM activity by KARI 201 on Aβ accumulation and many of the associated neuropathological features in vivo, we used the APP/PS1 mouse model. This AD mouse model is characterized by strong and progressive amyloid pathology with concomitant neuroinflammation (8, 30, 31), synapse and hippocampal neurogenesis loss (2, 32, 33), abnormal autophagy (8), and cognitive impairment (8, 30–32), similar to the disease progression observed in AD patients. Various doses (1, 5, or 10 mg·kg^{-1}) of KARI 201 were orally administered to 7.5-mo-old APP/PS1 mice. AMI (100 mg·kg^{-1}) was used to compare the therapeutic effects as previously reported (8) (Fig. 2*A*). Survival and body weight were not affected during administration of KARI 201 or AMI (Fig. 2 *B* and *C*). KARI 201–treated APP/PS1 mice exhibited dose-dependent reduction of ASM activity in plasma, cortex, and hippocampus compared with phosphate-buffered saline (PBS)–treated mice. Notably, the APP/PS1 mice treated with KARI 201 at a dose of 10 mg·kg^{-1} showed remarkable restoration of ASM activity to the normal range, a considerably greater effect compared with APP/PS1 mice treated with AMI at a dose of 100 mg·kg^{-1} (Fig. 2 *D*–*F*). This indicated the benefit of direct ASM inhibition by KARI 201. *Smpd1* mRNA and ASM protein levels were not changed by KARI 201 administration in APP/PS1 mice (*SI Appendix*, Fig. S10).

We next determined the Aβ profile. Thioflavin S and 6E10 staining, enzyme-linked immunosorbent assay (ELISA) of Aβ40 and Aβ42, and cerebral amyloid angiopathy revealed significantly lower Aβ levels in the brains of APP/PS1 mice treated with KARI 201 at a dose of 10 mg·kg^{-1} compared with the PBS- or AMI-treated groups (Fig. 2 *G*–*J*). In the KARI 201–treated mice, tau hyperphosphorylation also was reduced (Fig. 2*K*). To confirm the mechanism of decrease of Aβ accumulation, we assessed APP processing and the expression of the Aβ-generating enzyme Bace-1, but there were no significant differences by KARI 201 treatment (*SI Appendix*, Fig. S11). These results suggested that the inhibition of ASM activity by KARI 201 did not alter expression of APP and the Aβ-generating enzyme. We also performed Morris water maze testing and fear-conditioning studies, which showed that treatment with KARI 201 of 10 mg·kg^{-1} (Fig. 2 *L*–*R*) led to the greatest improvements in learning and memory. We further performed open-field and dark–light testing to examine locomotion and spontaneous activity. KARI 201–treated APP/PS1 mice exhibited an improved behavior pattern, similar to AMI-treated APP/PS1 mice (*SI Appendix*, Fig. S12). Thus, these results suggested that normalized ASM activity levels by KARI 201 administration, especially at 10 mg·kg^{-1}, reduced the Aβ load and improved learning and memory in APP/PS1 mice.

Synapse loss and neuroinflammation also are common neuropathological features that accompany Aβ accumulation in AD (2, 30, 31). To investigate the effects of KARI 201 on these neuropathological features, we performed immunolabeling for synaptophysin, PSD95, synapsin1, and MAP2 in cortex and hippocampus. Synapse loss, as observed in PBS-treated APP/PS1 mice, was improved by KARI 201 treatment (*SI Appendix*, Fig. S13). Moreover, highly activated microglia and astrocytes in cortex and hippocampus of PBS-treated APP/PS1 mice were significantly reduced in KARI 201–treated mice (*SI Appendix*, Fig. S14 *A* and *B*). Proinflammatory markers, including *Tnf*-α, *Il-1*β, *Il-6*, and *iNos*, and the immunoregulatory cytokine *Il-10* were decreased by KARI 201 treatment, while antiinflammatory markers, including *Il-4*, *Tgf*-β, and *Arg1*, increased compared with PBS-treated APP/PS1 mice (*SI Appendix*, Fig. S14*C*). Overall, these data revealed the significant therapeutic effects of the direct ASM inhibitor KARI 201 on Aβ accumulation and associated neuropathological features, such as synapse loss, neuroinflammation, and learning and memory impairment in the AD mouse model.

Neuronal ASM Inhibition by KARI 201 Rescues Autophagy Dysfunction and Microglial Phagocytic Function in APP/PS1 Mice. To further investigate the therapeutic mechanism of KARI 201, we assessed cell-specific ASM activity by KARI 201 treatment. Neurons, which are the main cell type impacted in AD pathogenesis, and microglia showed better improvement effects than astrocytes by KARI 201 treatment in cortex and hippocampus (*SI Appendix*, Fig. S14). PBS-treated APP/PS1 mice showed increased ASM activity in neurons derived from both cortex and hippocampus, but not in microglia, as observed in a previous study (8). In comparison, KARI 201–treated APP/PS1 mice exhibited restoration of ASM activity in these neurons. Consequently, elevated ceramide levels in neurons of APP/PS1 mice also were decreased by KARI 201 treatment. Although cortical and hippocampal microglia of PBS-treated APP/PS1 mice showed increased ceramide levels, this was not changed by KARI 201 treatment. We also confirmed whether KARI 201 impacted other sphingolipids, and did not find significant differences in neurons and microglia between the groups (*SI Appendix*, Fig. S15). Therefore, these results indicated that KARI 201 selectively inhibited neuronal ASM activity in cortex

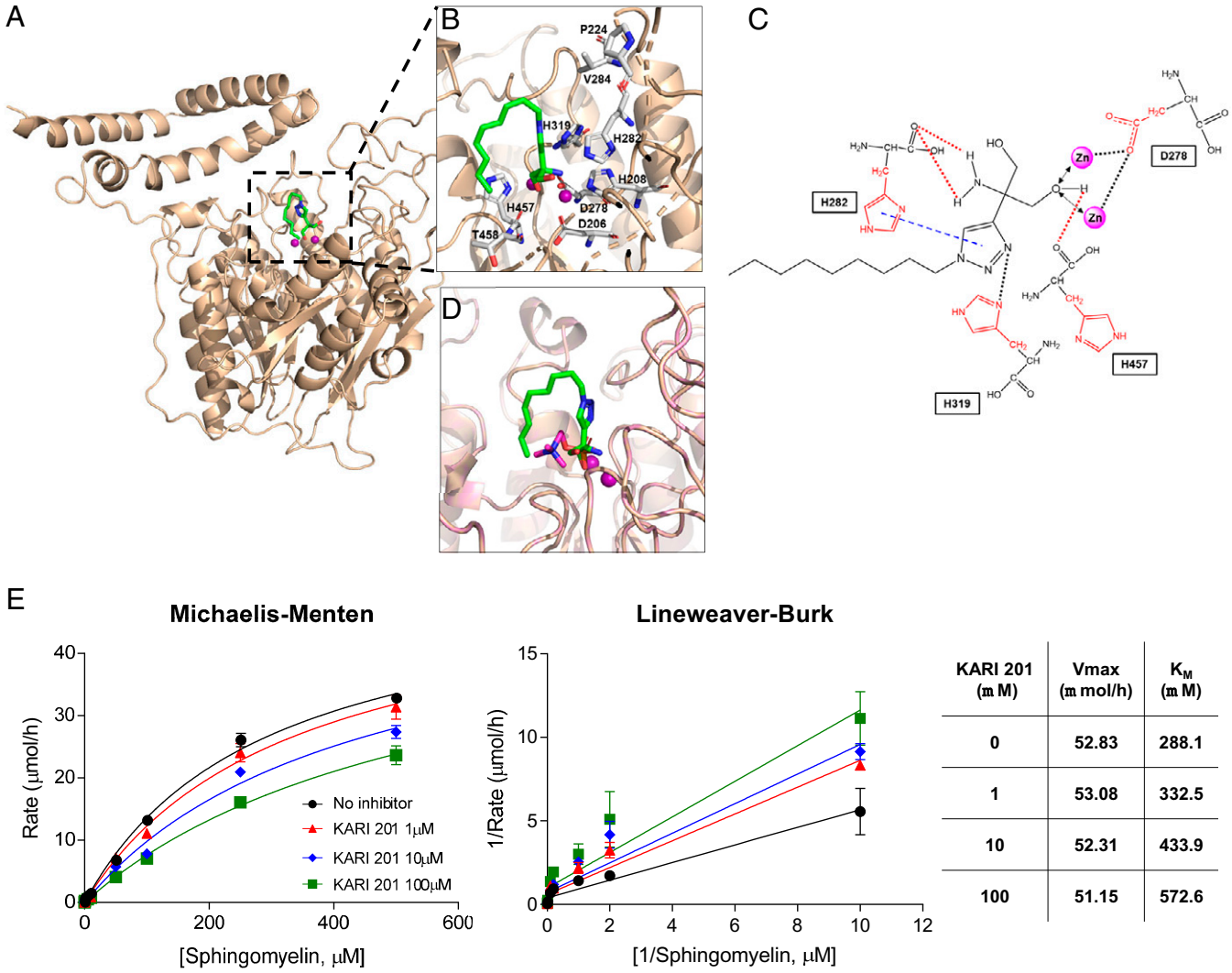

KARI 201 (㎛ M)	Vmax (㎛ mol/h)	K_M (㎛ M)
0	52.83	288.1
1	53.08	332.5
10	52.31	433.9
100	51.15	572.6

Fig. 1. KARI 201 is a competitive inhibitor that binds to the active site of ASM. (*A*) KARI 201 bound to the homology model of the cleft formed by the catalytic domain of ASM (Zn^{2+} ion denoted by a purple sphere). (*B*) Expanded view of KARI 201 within the orthosteric binding site (stick representation for the key residues). (*C*) Detailed interaction map between ASM and KARI 201. (*D*) Overlay of KARI 201 (green) and phosphocholine (purple) docked into the ASM binding site. (*E*) Biochemical mode of inhibition of KARI 201. Michaelis–Menten and Lineweaver–Burk plots show competitive inhibition between KARI 201 and sphingomyelin. Averages of three independent experiments are shown. $n = 3$ independent repeats.

and hippocampus of APP/PS1 mice, leading to reduced ceramide levels.

Previously, we reported that elevated neuronal ASM led to defective autophagic processing due to impaired lysosomal biogenesis in APP/PS1 mice (8). Particularly, the elevated neuronal ASM activity in APP/PS1 mice caused a defect of autophagic degradation but not induction (8). To examine whether ASM activity inhibition by KARI 201 could rescue autophagic degradation in neurons, we performed an autophagic flux assay through immunoblotting of microtubule-associated protein 1 light chain 3 (LC3)-II and p62 (8, 34). LC3-II levels are increased by overinduction of autophagy or reduction of autophagic turnover in the latter stages of autophagic degradation, while increased p62 is an indicator of autophagic turnover and represents defective autophagic degradation (8, 34). Serum starvation (which causes autophagic induction) enhanced LC3-II in neurons, which was further increased by the addition of ASM, indicating the combined effects of blocking autophagic degradation and enhancing induction (Fig. 3*A*). Moreover, the levels of p62 were similarly increased in neurons treated with ASM or NH_4Cl (which inhibits autophagic degradation), again showing that elevated ASM caused dysfunction of autophagic degradation but did not promote induction. Notably, KARI 201–treated neurons exhibited prevention of increased LC3-II and p62 in each setting, indicating improvement of the autophagic degradation (Fig. 3*A*). Defective autophagic degradation by ASM elevation is induced by defects in the autophagy-lysosome pathway (ALP) and lysosome biogenesis (8). Exogenous ASM was located in lysosomes of neurons, resulting in reduction of transcription factor EB (TFEB) and expression of lysosomal-associated membrane protein 1 (Lamp1), which are indicators of ALP function and lysosomal biogenesis (8, 35). The data showed decreased levels of TFEB and Lamp1 in ASM-treated neurons, but these levels were enhanced by KARI 201 treatment (Fig. 3 *B* and *C*). Additionally, ASM-treated neurons showed reduced

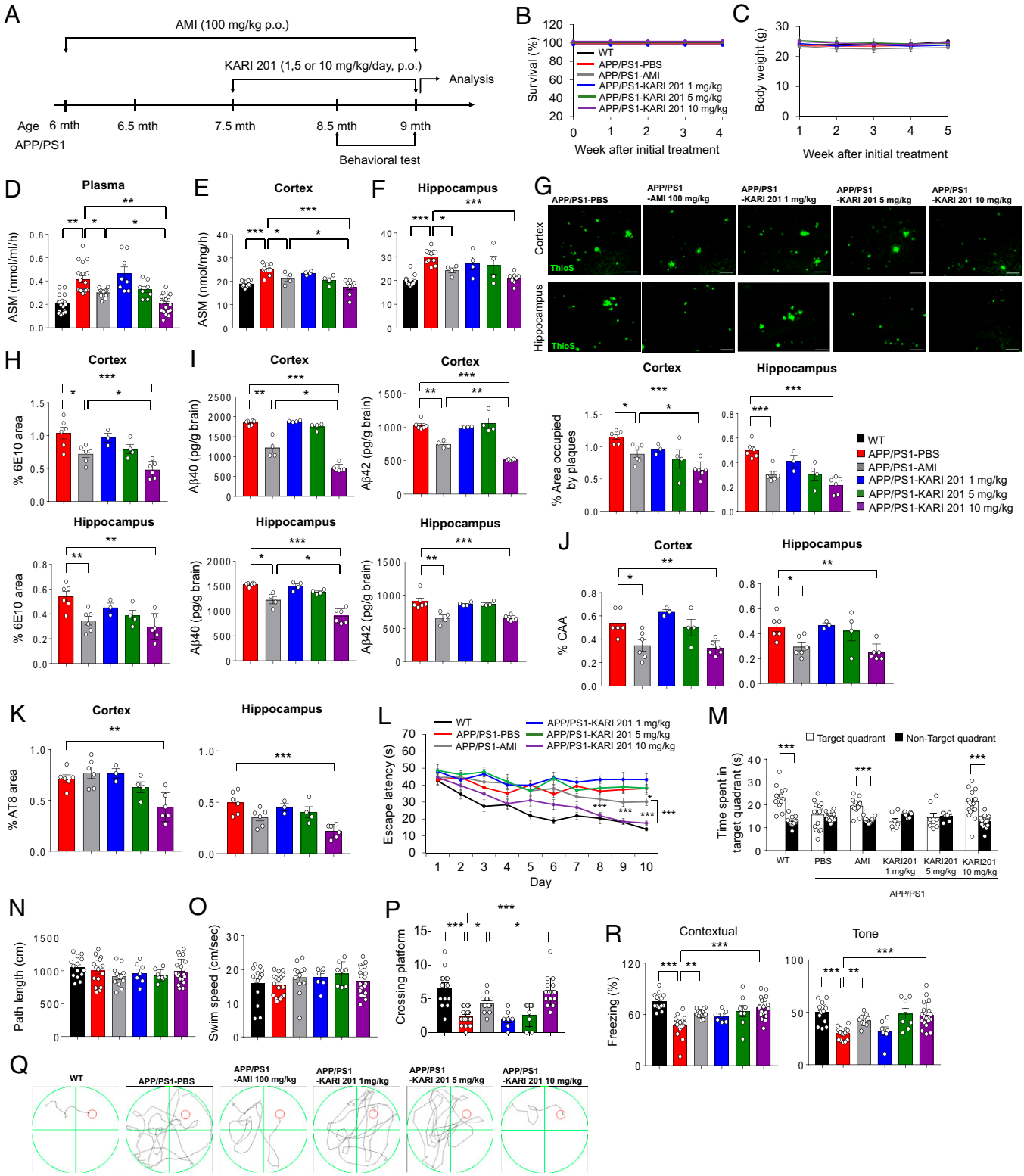

Fig. 2. Administration of KARI 201 reduces amyloid pathology and restores cognitive impairment in APP/PS1 mice. (*A*) Scheme of experimental procedures. (*B* and *C*) Survival (*B*) and body weight (*C*) during oral administration (p.o., per os) of each compound ($n = 8$ to 12 mice per group). (*D–F*) ASM activity in plasma (*D*; $n = 8$ to 18 mice per group), cortex (*E*; $n = 4$ to 11 mice per group), and hippocampus (*F*; $n = 4$ to 11 mice per group) of each group. (*G*, *Top*) Representative immunofluorescence images of thioflavin S (ThioS, Aβ plaques) in each group. (Scale bars, 100 μm.) (*G*, *Bottom*) Quantification of the area occupied by Aβ plaques ($n = 3$ to 6 mice per group). (*H*) Quantification of 6E10 ($n = 3$ to 6 mice per group). (*I*) Analysis of Aβ40 and Aβ42 depositions using ELISA kits ($n = 4$ to 6 mice per group). (*J* and *K*) Quantification of amyloid angiopathy (*J*; $n = 3$ to 6 mice per group; CAA) and tau hyperphosphorylation (*K*; $n = 3$ to 6 mice per group; AT8). (*L*) Learning and memory were assessed by the Morris water maze test ($n = 7$ to 19 mice per group). (*M–O*) At probe trial day 11, time spent on target platform (*M*), path length (*N*), and swim speed (*O*) were analyzed. (*P*) The number of times each animal entered the small target zone during the 60-s probe trial. (*Q*) Representative swimming paths at day 10 of training ($n = 7$ to 19 mice per group). (*R*) The results of contextual and tone tasks during fear-conditioning test ($n = 7$ to 19 mice per group). (*D–P* and *R*) One-way ANOVA, Tukey's post hoc test. $^*P < 0.05$, $^{**}P < 0.01$, $^{***}P < 0.001$. All error bars indicate SEM. All data analysis was done in 9-mo-old mice.

TFEB expression in the nuclear compartment compared with cytoplasm. The expression levels of TFEB-target genes related to the lysosome also were significantly decreased by ASM and improved by KARI 201 treatment (Fig. 3 *D* and *E*).

Next, to examine the in vivo effect of KARI 201 on autophagic dysfunction, we analyzed the expression of autophagy pathway indicators in the brains of wild-type (WT) and APP/PS1 mice treated with PBS or KARI 201. The levels of LC3-II and p62 were decreased both in cortex and hippocampus of KARI 201–treated APP/PS1 mice compared with PBS-treated APP/PS1 mice. Also, KARI 201 treatment significantly increased Lamp1 and TFEB protein levels with increased expression of TFEB-target genes (Fig. 3 *F–H*). We further measured the levels of beclin-1 (a part of the kinase complex responsible for autophagy induction) and cathepsin D (a lysosomal hydrolase) (8), and found that they did not vary between the groups. Thus, these findings suggested that inhibition of neuronal ASM activity by KARI 201 ameliorated the autophagic defect by restoring lysosomal biogenesis in APP/PS1 mice.

To explore whether the therapeutic effects of KARI 201 observed in the AD mouse model were similar in AD human neurons, we established induced pluripotent stem cells (iPSCs) with PS1 mutations and differentiated them into neurons (AD iPSC-derived neurons), as described in our previous studies (8, 30). ASM activity was significantly elevated in AD iPSC-derived neurons compared with normal iPSC-derived neurons, and was decreased by KARI 201 treatment in a time-dependent manner. The ceramide levels also were decreased in KARI 201–treated neurons, although the sphingomyelin levels were not changed (*SI Appendix*, Fig. S16 *A–C*). The decreased ASM activity by KARI 201 in AD iPSC-derived neurons was not due to down-regulation of *SMPD1* mRNA and ASM protein (*SI Appendix*, Fig. S16 *D* and *E*), indicating that KARI 201 directly inhibited ASM activity in AD patient neurons. Data on secretory ASM inhibition by KARI 201 in supernatant medium of AD iPSC-derived neurons or plasma of AD patients also supported this result (*SI Appendix*, Fig. S16 *F* and *G*). AD iPSC-derived neurons had significantly higher autophagic markers than normal iPSC-derived neurons, and KARI 201 treatment significantly restored the levels of these abnormal autophagic markers and increased expression of TFEB-target genes in AD iPSC-derived neurons, leading to decreased Aβ accumulation in these neurons (*SI Appendix*, Fig. S16 *H–J*). These results indicated that inhibition of ASM activity by KARI 201 led to decreased Aβ accumulation by restoring autophagic dysfunction in AD patient neurons.

In previous results, we observed improvement of microglial activation in cortex and hippocampus of KARI 201–treated APP/PS1 mice, despite the fact that ASM activity in microglia was not changed. These data supported the hypothesis that these improvements might be due to improvements in neuronal dysfunction mediated by autophagy normalization in the KARI 201–treated APP/PS1 mice. Several studies have demonstrated that neuronal damage mediated activated microglial morphology by releasing a variety of different signals (30, 36, 37). For example, "off" signals (*Cd47*, *Cx3cl1*, *Bdnf*, and *Cd200*) are responsible for keeping microglia in their resting state and antagonizing proinflammatory activity. In contrast, "on" signals (*Cxcl10*, *Ccl21*, and *Mmp3*) are present under conditions of neuronal damage and can initiate detrimental microglial function (36). To test whether restoration of autophagic dysfunction by KARI 201 neurons regulated microglial function through off/on signals, we assessed these molecules in cortex and hippocampus of WT and APP/PS1 mice treated with PBS or KARI 201 and found that alteration of these molecules in PBS-treated APP/PS1 mice was improved by KARI 201 (*SI Appendix*, Fig. S17*A*). We next examined the change of microglial phagocytic function in these mice, and found that microglial recruitment surrounding Aβ was increased in KARI 201–treated APP/PS1 mice compared with PBS-treated APP/PS1 mice (*SI Appendix*, Fig. S17*B*). These mice also showed an increased number of microglia containing costained lysosomes and Aβ. Additionally, the morphology of microglia, closely related to this function, displayed phagocytic amoeboid morphology in KARI 201–treated APP/PS1 mice (*SI Appendix*, Fig. S17 *C* and *D*). Consequently, the KARI 201–treated mice exhibited increased levels of smaller Aβ species (<25 μm) and decreased levels of larger Aβ aggregates (25 to 50 μm, >50 μm), compared with those of the PBS-treated APP/PS1 mice (*SI Appendix*, Fig. S17*E*). Thus, it could be inferred that improvement of the autophagic defect in neurons of APP/PS1 mice by the ASM inhibitor of KARI 201 led to enhancement of phagocytic function of microglia. In addition, restoration of neuronal autophagy and microglial function by KARI 201 might lead to synergistic effects on Aβ degradation in APP/PS1 mice.

KARI 201 Is Also a Ghrelin Receptor Agonist, Contributing to Improvement of Neuropathological Features in Hippocampus of APP/PS1 Mice. To further investigate the regulation of neurons and microglia by KARI 201, we analyzed the gene expression patterns of cortical neurons and microglia derived from WT and APP/PS1 mice treated with PBS or KARI 201 using RNA-seq. Importantly, the altered expression of several genes observed in both cortical neurons and microglia of PBS-treated APP/PS1 mice was normalized in KARI 201–treated APP/PS1 mice (*SI Appendix*, Figs. S18*A* and S19*A*). Notably, we found that cortical neurons and microglia isolated from PBS-treated APP/PS1 mice expressed high levels of genes related to translation (e.g., neurons: *Rpl11*, *Rpl12*, *Rpl17*, *Rpl31*, *Rpl32*, *Rpl34-ps1*, *Rpl36a*, *Rpl4*, *Rps20*, *Rps23*, *Rps24*, *Rps27a*, and *Rps7*; microglia: *Rpl24*, *Rpl27a*, *Rpl35*, *Rpl36*, *Rps11*, *Rps14*, *Rps26*, *Rps28*, and *Rps29*) compared with WT cells (with <2 *Z* score and $P < 0.05$). Altered or dysfunctional ribosomal proteins encoded by these genes have recently been shown to contribute to neuropathological features of various neurodegenerative disorders, including AD (38–40), such as neuronal loss (38, 39), defective synaptic plasticity (38), inflammation (41, 42), and abnormal protein aggregation (38, 40). Interestingly, the abnormal up-regulated expression of these genes was restored in KARI 201–treated APP/PS1 mice in cortical neurons and microglia, indicating that KARI 201 could regulate the translational machinery, including ribosomal proteins and associated factors necessary for protein biosynthesis. In this regard, functional categorization using the DAVID bioinformatics database for Gene Ontology term enrichment analysis (biological process and molecular function) also showed the association with translation and structural constituents of the ribosome (*SI Appendix*, Figs. S18 *B* and *C* and S19 *B* and *C*). Kyoto Encyclopedia of Genes and Genomes pathway analysis further identified a considerable enrichment of ribosomal genes in both cell types (*SI Appendix*, Figs. S18*D* and S19*D*).

Previous studies suggested that GPCRs impact the translational machinery and subsequent mRNA translation (43, 44). GPCRs exert their physiological function by transducing a complex signaling network that coordinates gene expression. In this process, translation responds to the signaling network generated by extracellular signals targeting GPCRs, leading to protein synthesis that broadly impacts physiological function (43, 44). This observation led us to focus on the possible interaction between GPCRs and KARI 201. This interaction was supported by our data exhibiting the restoration of gene expression related to regulation of G protein signaling both in cortical neurons (e.g., *Rgs9*, *Rgs10*, and *Rgs14*) and microglia (e.g., *Rgs9* and *Rgs11*) of KARI 201–treated APP/PS1 mice.

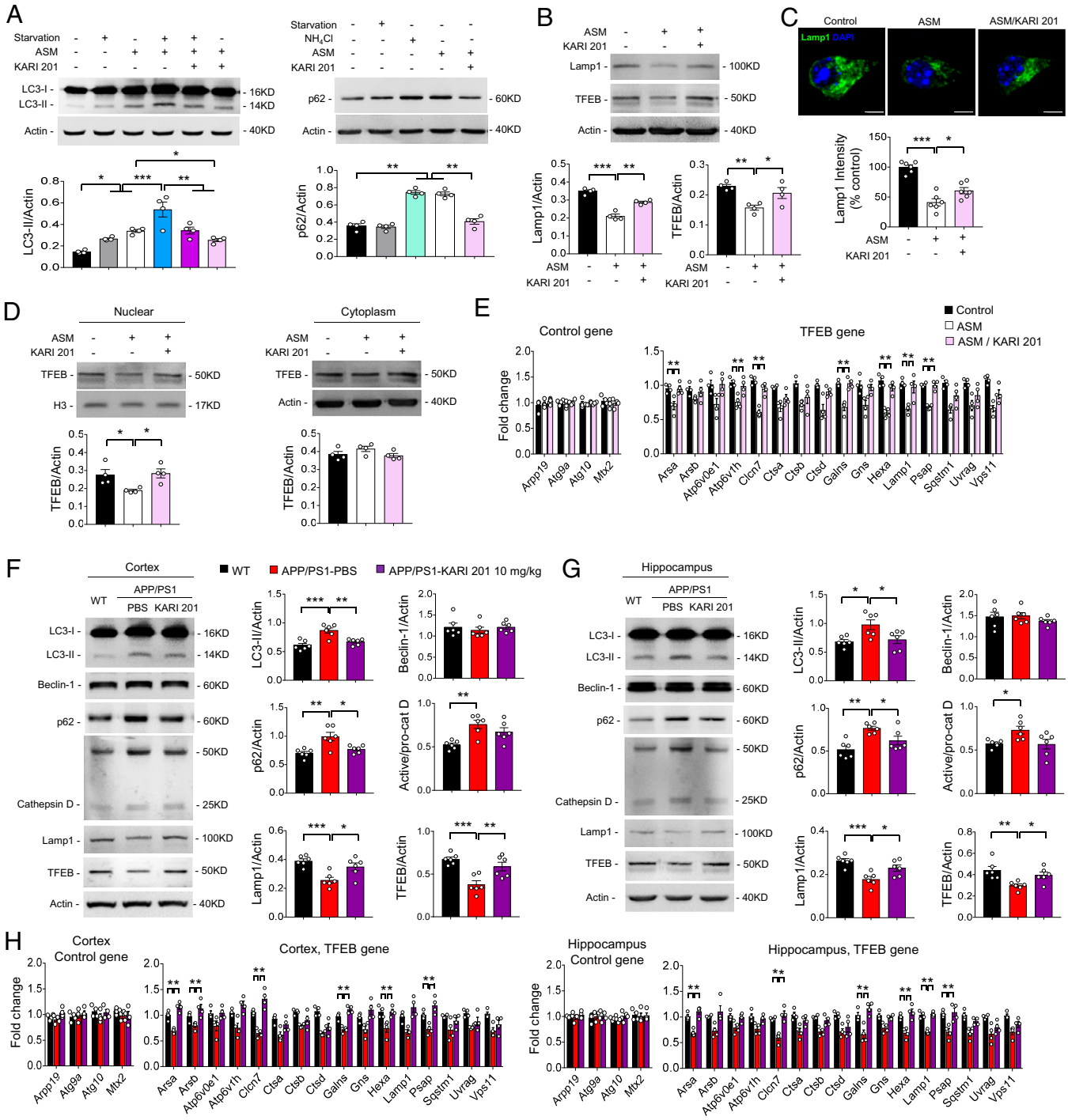

Fig. 3. KARI 201 ameliorates defective autophagy degradation by regulating lysosomal biogenesis in neurons. (*A*) Autophagic flux assay. Mouse neurons were cultured in medium with or without ASM (10 μM) or KARI 201 (10 μM) under complete medium or starvation conditions. The LC3-II levels were examined by Western blotting. The accumulation of p62 was assessed with ASM (10 μM), KARI 201 (10 μM), NH_4Cl (20 mM), or starvation (n = 4 per group). (*B*) The levels of TFEB and Lamp1 in mouse neurons (n = 4 per group). (*C*) Immunocytochemistry of Lamp1 in ASM-treated cells with or without KARI 201 (n = 6 per group). (Scale bars, 5 μm.) (*D*) Western blot analysis for nuclear localization of TFEB in ASM-treated cells with or without KARI 201 (n = 4 per group). (*E*) qRT-PCR analysis of TFEB-target gene expression in each group (n = 4 per group). (*F* and *G*) Western blot analyses and quantification for LC3, Beclin-1, p62, cathepsin D, Lamp1, and TFEB in cortex (*F*) and hippocampus (*G*) in WT and APP/PS1 mice treated with PBS or KARI 201 (n = 6 mice per group). (*H*) The expression of TFEB-target genes in each group (n = 4 mice per group). One-way ANOVA, Tukey's post hoc test. *P < 0.05, **P < 0.01, ***P < 0.001. All error bars indicate SEM. All data analysis was done in 9-mo-old mice.

Based on previous reports and our RNA-seq data, we performed GPCR screening against 170 GPCRs at 10 μM KARI 201. We considered results significant when inhibition or stimulation by the drug was higher than 50%. Surprisingly, we found that KARI 201 had a highly potent effect (83.7%) as a ghrelin receptor (GHSR1α) agonist (Fig. 4). These findings suggested that KARI 201 might restore the alteration of gene expression related to translation via interaction with GPCR (ghrelin

receptor) in cortical neurons and microglia of APP/PS1 mice. GHSR1α has been known to be involved in various physiological functions by binding to ghrelin (21–23). In the brain, GHSR1α is abundantly expressed in hypothalamus and hippocampus (22, 45). Ghrelin/GHSR1α signaling in hypothalamus regulates orexigenic effects (46), and in hippocampus it contributes to hippocampal synaptic function and neurogenesis (21–23). Therefore, several studies have demonstrated the therapeutic implications of hippocampal ghrelin/GHSR1α signaling in learning and memory for AD (21–23, 47). After identifying the role of KARI 201 as a ghrelin receptor agonist, we investigated whether this activity could be responsible for improved hippocampal synaptic function and neurogenesis in the AD mouse model. First, we reconfirmed the effect of KARI 201 as a GHSR1α agonist on Ca^{2+} mobilization in HEK293A cells that overexpressed GHSR1α. KARI compounds, including KARI 201, and ghrelin (positive control) were added to these cells, and we observed that KARI 201 and KARI 101, but not the other compounds, produced a strong agonist effect (Fig. 5*A*). These results might be related to the number of carbons in the chains on the compounds and their ability to bind GHSR1α, similar to the direct ASM inhibition effects. Analysis of major downstream (AMPK, PI3K, and ERK) targets of ghrelin/GHSR1α signaling revealed only activation of AMPK (adenosine monophosphate–activated protein kinase), which is highly related to Ca^{2+} release (21, 22), in KARI 201–treated cells (Fig. 5*B*). The effects of KARI 201 on GHSR1α internalization, a characteristic of receptor desensitization, also was examined. Internalization of GHSR1α was observed after treatment with KARI 201 and KARI 101, as shown in ghrelin-treated cells (Fig. 5*C*). Therefore, these data suggested that KARI 201 and KARI 101 could play a role as GHSR1α agonists.

Next, we evaluated whether GHSR1α activation by KARI 201, which had significantly better pharmacological properties than KARI 101, could restore hippocampal neurogenesis and synaptic function in Aβ environments. We applied KARI 201 to oligomeric Aβ42-exposed mouse hippocampal neural stem cell (NSC) cultures, and the number of neurospheres was counted and Edu assays were performed to test self-renewal function and proliferation capacity. The decrease of these functions by Aβ42 was restored by KARI 201 treatment, and the levels of neuronal survival genes (*Map2*, *Gap43*, *Mbp*, and *Tuj1*) also were increased (Fig. 5 *D*–*F*). Moreover, we confirmed increased synaptic density in oligomeric Aβ42-treated mouse or human hippocampal neurons with KARI 201 treatment (Fig. 5*G*). These results indicated that GHSR1α activation by KARI 201 promoted hippocampal neurogenesis and synaptic formation in Aβ42-exposed neurons.

A previous study has reported that elevated ASM could contribute to decreased hippocampal neuronal proliferation and survival by increasing ceramide production (13). To directly test this, we measured ASM activity and ceramide levels in oligomeric Aβ42-treated mouse hippocampal NSCs or neurons with and without KARI 201 treatment. ASM activity and ceramide levels were increased by Aβ42 treatment in both cells, and were reduced by KARI 201 treatment (Fig. 5*H*), suggesting that dual action of KARI 201 as a GHSR1α agonist and ASM activity inhibitor might impact the restoration of hippocampal NSC function and synaptic loss. We also further confirmed improvement of hippocampal dysfunction by KARI 201 in APP/PS1 mice by additional analyses. KARI 201–treated APP/PS1 mice showed a significant increase of $Ki67^+$ proliferating cells, immature neurons ($BrdU^+/DCX^+$ cells), and neural progenitors ($SOX2^+/S100\beta^-$ cells) in dentate gyrus of hippocampus compared with PBS-treated APP/PS1 mice (Fig. 5 *I*–*K*). The cells detected by c-Fos, which is associated with changes in neuronal gene expression that promote learning and memory function (23, 48), also were increased by KARI 201 treatment in APP/PS1 mice (Fig. 5*L*). Long-term potentiation (LTP) induction of the hippocampal Schaffer collateral–CA1 pathway elicited by high-frequency stimulation (HFS) has been proposed as a candidate for the cellular mechanism of learning and memory. KARI 201 increased hippocampal LTP in the CA1 region of WT mice compared with control WT mice, and also improved expression in APP/PS1 mice (Fig. 5 *M* and *N*). These findings indicated that KARI 201 promoted hippocampal synaptic plasticity and that this might benefit learning and memory in normal and even AD mice.

In support of these results, comparative RNA-seq analysis surprisingly showed that KARI 201 treatment restored the alteration of gene expression (*Gpr88*, *Meis2*, *Npas2*, *Nrtn*, and *Ptgs2*) associated with learning, behavior, cognition, and memory in hippocampus of APP/PS1 mice (*SI Appendix*, Fig. S20). These findings strongly suggested a role of KARI 201 as a GHSR1α agonist in AD hippocampal neurogenesis and synaptic improvement, and also indicated that combined action of GHSR1α activation and ASM activity inhibition by KARI 201 could effectively rescue hippocampal memory impairment in AD.

Finally, to reconfirm the therapeutic effects of KARI 201, we repeated these studies in another mouse model of AD, 5xFAD mice, and found that KARI 201 treatment inhibited ASM activity in plasma, cortex, and hippocampus in 5xFAD mice, leading to improvement of Aβ accumulation and associated neuropathological features, including autophagy dysfunction, microglial phagocytosis, synapse loss, and reduction of hippocampal neurogenesis and neuronal activity (*SI Appendix*, Figs. S21 and S22). Collectively, these results demonstrated that KARI 201 treatment efficiently attenuated Aβ accumulation and other neuropathological features, including memory impairment, by its dual activity in neurons as an ASM direct inhibitor and GHSR1α agonist.

Discussion

Considering the many complex pathologic processes in AD, multitargeted therapeutic approaches are advantageous for effective AD treatment. In this study, we focused on identifying an efficient, direct inhibitor of ASM activity based on previous studies demonstrating the importance of this enzyme for the development of various neuropathological features in AD. Our efforts led to the discovery of the KARI series of inhibitors. Further analysis led to optimization of the shared KARI backbone by the addition of 6- to 10-carbon chains. This optimization strategy was performed to enhance lipophilicity for effective BBB penetration in AD (24, 25). Interestingly, a longer length of carbon chain correlated with higher ASM binding and inhibitory effects. Moreover, we observed that the bioavailability, brain distribution, and microsomal stability were also dependent on the number of carbons in the alkyl chain. These findings indicated that the length of the carbon chain in the compound might play a critical role for stable binding to ASM and enhanced PK properties, especially brain distribution, leading us to select KARI 201, with a 9-carbon chain, the most optimal compound with these properties.

We found that KARI 201 was a highly selective and direct ASM activity inhibitor without off-target effects. Furthermore, KARI 201 showed selective inhibition of ASM activity in neurons of AD mice, and restored autophagy dysfunction by improving lysosomal biogenesis. The normalized neuronal autophagic function in KARI 201–treated AD mice led to enhancement of the Aβ phagocytic function of microglia, resulting in improvements of Aβ deposit, neuroinflammation, synapse plasticity, and memory dysfunction (*SI Appendix*, Fig. S23*A*). These results suggested that KARI 201 could be a

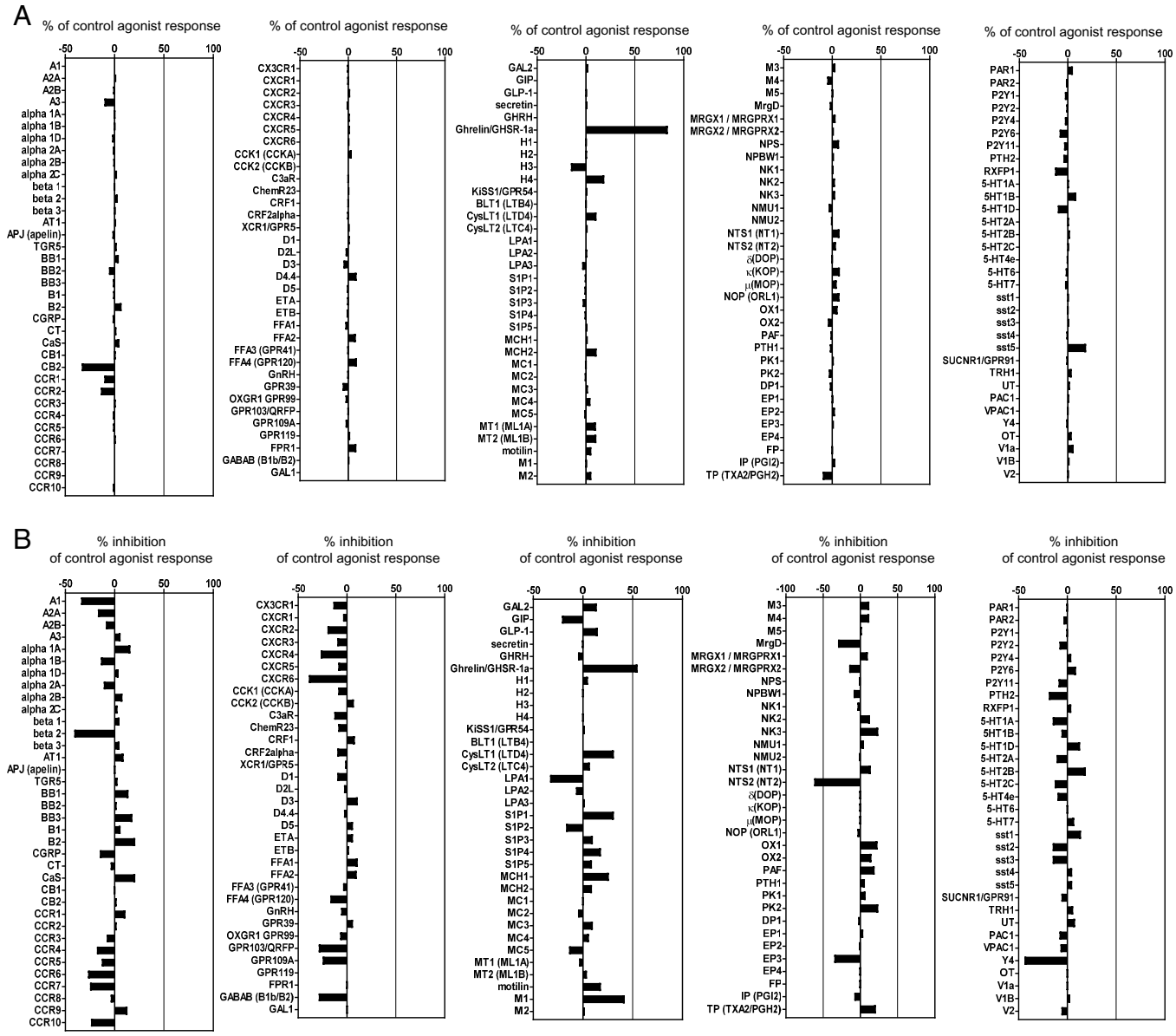

Fig. 4. GPCR screening of KARI 201 was performed at 10 μM concentration. The results are expressed as a percent of control agonist response (*A*) or inverse agonist response (measured response/control response × 100, average of two duplicate determinations) and as a percent inhibition of control agonist response (*B*) (100 − (measured response/control response × 100), average of two duplicate determinations). KARI 201 had an effect as a ghrelin receptor agonist (83.7% of control agonist response). All error bars indicate SEM.

compound that might be useful for targeting several of the neuropathological features in AD.

RNA-seq analysis in cortex of AD mice also unexpectedly revealed the possibility of interaction between GPCRs and KARI 201. We went on to identify a role for KARI 201 as a ghrelin receptor agonist via GPCR screening. Several studies have highlighted the importance of ghrelin/ghrelin receptor signaling in the hippocampal synaptic physiology associated with memory in AD (21–23, 47), although current therapeutic efforts using ghrelin for AD treatment have not been effective in correcting hippocampal synaptic deficits and memory impairment. Ghrelin levels are known to be elevated in plasma of AD patients (49), and this might lead to ghrelin resistance and the need for high doses of ghrelin in clinical studies. However, high doses of ghrelin might contribute to tumor growth, as it increases the levels of growth hormone and insulin-like growth factor-1, both of which stimulate tumor growth (50). Therefore, the use of ghrelin receptor agonists is a logical alternative to using ghrelin directly in clinical practice. We observed that KARI 201 and KARI 101 both acted as ghrelin receptor agonists, but not the other three KARI compounds in our test group. This might be related to the carbon chain length of the compound in binding to the ghrelin receptor, similar to ASM binding, and the data indicated that chain lengths of 9 carbons or more provided optimal binding to the ghrelin receptor. Ghrelin is a 28–amino acid peptide that is acylated at its third serine residue with an octanoyl group (51). Recently, it has been reported that the octanoyl chain of ghrelin plays a critical role in binding to the receptor, supporting our results (52, 53). Based on our findings and recent reports, we suggest that

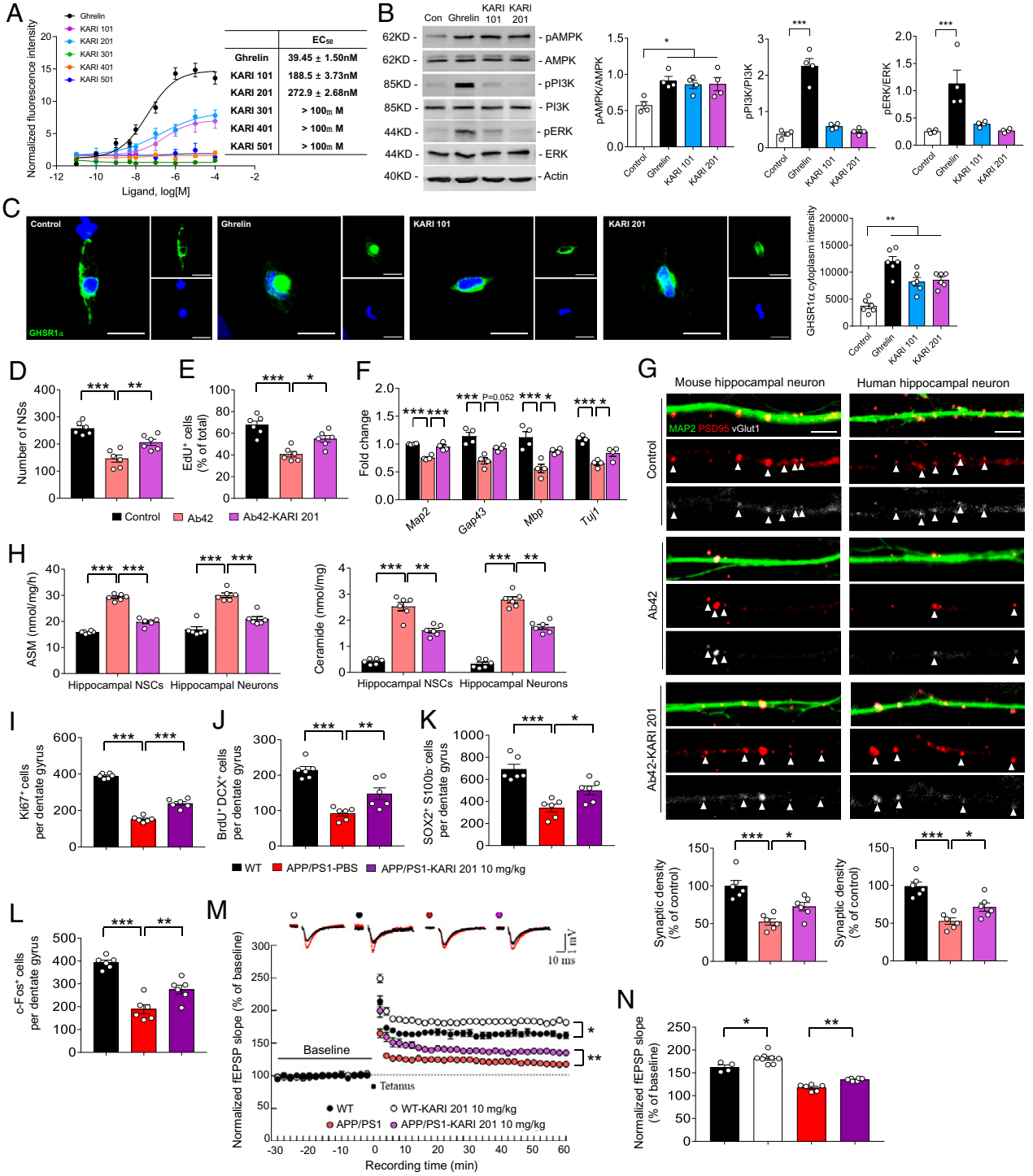

Fig. 5. KARI 201 is a ghrelin receptor agonist and improves hippocampal neurogenesis and synapse plasticity. (*A*) Effect of various concentrations of the KARI compounds and ghrelin on Ca^{2+} mobilization in HEK293 cells transiently transfected with the WT human GhrR (data are mean ± SEM; $n = 3$ independent experiments). (*B*) Western blot analyses and quantification of pAMPK, APMK, pPI3K, PI3K, pERK, and ERK in ghrelin (10 μM), KARI 101 (10 μM), or KARI 201 (10 μM) treatment ($n = 4$ per group). (*C*) Immunocytochemistry of the ghrelin receptor ($n = 6$ per group). (Scale bars, 20 μm.) (*D* and *E*) Number of neurospheres (NSs) (*D*) and EdU-positive NSCs (*E*) in Aβ42 (1 μM, 24 h) treatment with or without KARI 201 ($n = 6$ per group). (*F*) qRT-PCR analysis of neuronal survival gene expression ($n = 4$ per group). (*G*) Effect of KARI 201 treatments on synaptic density in mouse hippocampal neurons in the presence or absence of Aβ42. Quantification and representative images of synapse staining. vGlut1 (white) and PSD95 (red) were used to visualize pre- and postsynaptic terminals, respectively. The dendrites were stained with MAP2 (green). The overlaid staining of vGlut1/PSD95 identifies synapses ($n = 6$ per group). (Scale bars, 5 μm.) (*H*) ASM activity and ceramide production in NSCs and neurons in Aβ42 treatment with or without KARI 201 ($n = 6$ per group). (*I–K*) The number of $Ki67^+$ cells (*I*, proliferating cells), $BrdU^+/DCX^+$ cells (*J*, new neuroblasts), and $SOX2^+/S100\beta^-$ cells (*K*, NSCs) in dentate gyrus of each mouse ($n = 6$ mice per group). (*L*) The number of c-Fos^+ neurons in dentate gyrus of each mouse ($n = 6$ mice per group). (*M* and *N*) LTP induced by HFS (WT, $n = 4$; WT/KARI 201, 10 mg·kg^{-1}, $n = 8$; APP/PS1/PBS, $n = 4$ to 6; APP/PS1/KARI 201, 10 mg·kg^{-1}, $n = 6$). (*B–N*) One-way ANOVA, Tukey's post hoc test. $^*P < 0.05$, $^{**}P < 0.01$, $^{***}P < 0.001$. All error bars indicate SEM. All data analysis was done in 9-mo-old mice.

further studies are needed to more specifically characterize the binding action of KARI 201 and KARI 101 with the ghrelin receptor.

The action of KARI 201 as a ghrelin receptor agonist induced Ca^{2+} influx and downstream activation of AMPK. In previous studies, AMPK activation has been reported to be involved in improvement of hippocampal neurogenesis by increasing transcription of proneurogenesis genes such as BDNF (brain-derived neurotrophic factor) (22, 54). We also observed increased BDNF expression in the brain of KARI 201–treated AD mice. Furthermore, KARI 201 restored the loss of hippocampal neurogenesis and synapse plasticity in Aβ-exposed NSCs, neurons, and AD mice. The effects on mitigation of hippocampal neurogenesis could also result from ceramide reduction by ASM activity inhibition, and these combined effects of KARI 201 contributed to an overall effective improvement of hippocampal memory impairment of AD mice (*SI Appendix*, Fig. S23*B*).

Numerous studies have reported that ghrelin agonists improve diverse AD-related neuropathological features (21–23, 47, 54), similar to ASM inhibition. For example, ghrelin receptor stimulation through ghrelin and its analogs promotes the autophagic degradation of Aβ-containing autophagosomes by regulating autophagy mediators through the AMPK pathway. This pathway also reduces abnormal hyperphosphorylation of tau by phosphorylating GSK-3β (21, 22). Moreover, the activation of the ghrelin receptor prevents neuroinflammation, although the majority of studies suggest that this effect is indirect and through its cytoprotective properties in neurons and other cerebral cells (21, 22). Hence, targeting the ghrelin receptor could be an efficient therapeutic strategy for neuropathological features in AD, similar to targeting ASM inhibition (*SI Appendix*, Fig. S23*B*). We also suggest that the therapeutic effects of KARI 201 as a ghrelin receptor agonist are more dominant in hippocampus because the expression of the ghrelin receptor is more abundant in hippocampus than other brain regions (22), while the effects of KARI 201 as an ASM inhibitor are broader and include cortex and other regions.

Chronic systemic inflammation is one of the important pathological features in AD (7, 21). Aggregated amyloids or fragments of apoptotic neurons may reach the circulatory stream following BBB breaching, leading to subsequent peripheral inflammatory responses by antigen-presenting cells and lymphocytes (T cells) and resulting in immune cell entry into the brain in AD (21, 55, 56). In the process of immune cell infiltration, proinflammatory immune cells enhance BBB disruption and exacerbate neuroinflammation (55, 56). Several studies reported that ASM inhibition and ghrelin receptor activation could both have beneficial effects on peripheral inflammation, as well as BBB abnormalities (14–17, 21, 22). We previously reported ASM-mediated BBB disruption (14) and others demonstrated pathogenic T cell activation by ASM (16), suggesting that ASM inhibition might contribute to improvement of BBB damage and systemic inflammation. The activation of the ghrelin receptor also suppresses proinflammatory immune cells and blocks immune cell invasion into the brain, resulting in the prevention of inflammation-driven permeabilization of the BBB (21, 22). Thus, we propose that KARI 201 acts as both an ASM inhibitor and ghrelin receptor agonist to improve the systemic pathological features of AD (*SI Appendix*, Fig. S23*C*).

Collectively, the fact that ASM and the ghrelin receptor in neurons are both considered valuable therapeutic targets for Aβ deposit and other neuropathological features in AD indicates that KARI 201 could be a potential multifaceted drug with excellent pharmacological properties for therapeutic application in AD. Further, the combination of KARI 201 with current therapeutic agents such as anti-Aβ and tau antibodies might present synergetic effects in improvement of several AD-related neuropathological features. However, we are aware of the limitations of using AD mouse and cell models for drug development, and that many drugs which have been efficacious in these model systems have not been effective in humans. Nonetheless, many of the neuropathological features observed in these models are associated with human AD, and we believe that KARI 201 may be a promising drug for AD and perhaps other neurologic diseases in which ASM activity is increased or ghrelin receptor signaling is dysregulated. For this, further preclinical and clinical studies should be carried out in the future.

Materials and Methods

Chemical Compound Screening. Chemical compounds (1,273) from a sphingolipid-targeted library and a FIASMA derivative–targeted library were tested in triplicate assays at 10 μM compound (stock at 50 mM diluted in dimethyl sulfoxide) for 30 min in PS1 fibroblasts with an abundant ASM activity. An ultra-performance liquid chromatography system (Waters) was used for analysis of ASM activity. The common backbone of compounds with a percent inhibition >30% was identified and further optimization was performed based on lipophilicity. Hits were further qualified through direct binding to ASM by SPR, confirmation of direct and selective ASM inhibition in biochemical and cellular assays, pharmacokinetics, drug ability, and in vivo efficacy. The details of experimental protocols and analytical methods are presented in *SI Appendix*.

Data Availability. All study data are included in the article and/or *SI Appendix*.

ACKNOWLEDGMENTS. The chemical library used in this study was kindly provided by the Korea Chemical Bank of the Korea Research Institute of Chemical Technology. This work was supported by National Research Foundation of Korea grants funded by the Korean government (MSIT) (2020R1A4A2002691, 2020R1A2C3006875, 2020R1A2C3006734). This research was also supported by a grant of the Korea Health Technology R&D Project through the Korea Health Industry Development Institute, funded by the Ministry of Health & Welfare and MSIT, Republic of Korea (HU20C0345).

1. R. Donev, M. Kolev, B. Millet, J. Thome, Neuronal death in Alzheimer's disease and therapeutic opportunities. *J. Cell. Mol. Med.* **13**, 4329–4348 (2009).
2. G. Kashyap *et al.*, Synapse loss and progress of Alzheimer's disease—A network model. *Sci. Rep.* **9**, 6555 (2019).
3. O. Lazarov, M. P. Mattson, D. A. Peterson, S. W. Pimplikar, H. van Praag, When neurogenesis encounters aging and disease. *Trends Neurosci.* **33**, 569–579 (2010).
4. M. S. Uddin *et al.*, Autophagic dysfunction in Alzheimer's disease: Cellular and molecular mechanistic approaches to halt Alzheimer's pathogenesis. *J. Cell. Physiol.* **234**, 8094–8112 (2019).
5. J. Shi, G. Perry, M. A. Smith, R. P. Friedland, Vascular abnormalities: The insidious pathogenesis of Alzheimer's disease. *Neurobiol. Aging* **21**, 357–361 (2000).
6. M. D. Sweeney, A. P. Sagare, B. V. Zlokovic, Blood-brain barrier breakdown in Alzheimer disease and other neurodegenerative disorders. *Nat. Rev. Neurol.* **14**, 133–150 (2018).
7. S. Amor, M. N. Woodroofe, Innate and adaptive immune responses in neurodegeneration and repair. *Immunology* **141**, 287–291 (2014).
8. J. K. Lee *et al.*, Acid sphingomyelinase modulates the autophagic process by controlling lysosomal biogenesis in Alzheimer's disease. *J. Exp. Med.* **211**, 1551–1570 (2014).
9. J. Kornhuber, C. Rhein, C. P. Müller, C. Mühle, Secretory sphingomyelinase in health and disease. *Biol. Chem.* **396**, 707–736 (2015).
10. W. Y. Ong, D. R. Herr, T. Farooqui, E. A. Ling, A. A. Farooqui, Role of sphingomyelinases in neurological disorders. *Expert Opin. Ther. Targets* **19**, 1725–1742 (2015).
11. R. W. Jenkins, D. Canals, Y. A. Hannun, Roles and regulation of secretory and lysosomal acid sphingomyelinase. *Cell. Signal.* **21**, 836–846 (2009).
12. E. L. Smith, E. H. Schuchman, The unexpected role of acid sphingomyelinase in cell death and the pathophysiology of common diseases. *FASEB J.* **22**, 3419–3431 (2008).
13. E. Gulbins *et al.*, Acid sphingomyelinase-ceramide system mediates effects of antidepressant drugs. *Nat. Med.* **19**, 934–938 (2013).
14. M. H. Park *et al.*, Vascular and neurogenic rejuvenation in aging mice by modulation of ASM. *Neuron* **100**, 167–182.e9 (2018).
15. H. Y. Chung *et al.*, Acid sphingomyelinase promotes endothelial stress response in systemic inflammation and sepsis. *Mol. Med.* **22**, 412–423 (2016).
16. A. Bai, Y. Guo, Acid sphingomyelinase mediates human $CD4^+$ T-cell signaling: Potential roles in T-cell responses and diseases. *Cell Death Dis.* **8**, e2963 (2017).
17. M. H. Park, H. K. Jin, J. S. Bae, Potential therapeutic target for aging and age-related neurodegenerative diseases: The role of acid sphingomyelinase. *Exp. Mol. Med.* **52**, 380–389 (2020).

18. C. Arenz, Small molecule inhibitors of acid sphingomyelinase. *Cell. Physiol. Biochem.* **26**, 1–8 (2010).
19. E. Naser *et al.*, Characterization of the small molecule ARC39, a direct and specific inhibitor of acid sphingomyelinase in vitro. *J. Lipid Res.* **61**, 896–910 (2020).
20. K. Yang *et al.*, Discovery of potent, selective, and direct acid sphingomyelinase inhibitors with antidepressant activity. *J. Med. Chem.* **63**, 961–974 (2020).
21. N. Reich, C. Hölscher, Acylated ghrelin as a multi-targeted therapy for Alzheimer's and Parkinson's disease. *Front. Neurosci.* **14**, 614828 (2020).
22. S. G. Jeon *et al.*, Ghrelin in Alzheimer's disease: Pathologic roles and therapeutic implications. *Ageing Res. Rev.* **55**, 100945 (2019).
23. A. K. E. Hornsby *et al.*, Unacylated-ghrelin impairs hippocampal neurogenesis and memory in mice and is altered in Parkinson's dementia in humans. *Cell Rep. Med.* **1**, 100120 (2020).
24. N. H. Greig, S. Genka, E. M. Daly, D. J. Sweeney, S. I. Rapoport, Physicochemical and pharmacokinetic parameters of seven lipophilic chlorambucil esters designed for brain penetration. *Cancer Chemother. Pharmacol.* **25**, 311–319 (1990).
25. R. N. Waterhouse, Determination of lipophilicity and its use as a predictor of blood-brain barrier penetration of molecular imaging agents. *Mol. Imaging Biol.* **5**, 376–389 (2003).
26. R. Hurwitz, K. Ferlinz, K. Sandhoff, The tricyclic antidepressant desipramine causes proteolytic degradation of lysosomal sphingomyelinase in human fibroblasts. *Biol. Chem. Hoppe Seyler* **375**, 447–450 (1994).
27. Y. F. Zhou *et al.*, Human acid sphingomyelinase structures provide insight to molecular basis of Niemann-Pick disease. *Nat. Commun.* **7**, 13082 (2016).
28. A. Gorelik, K. Illes, L. X. Heinz, G. Superti-Furga, B. Nagar, Crystal structure of mammalian acid sphingomyelinase. *Nat. Commun.* **7**, 12196 (2016).
29. Z. J. Xiong, J. Huang, G. Poda, R. Pomès, G. G. Privé, Structure of human acid sphingomyelinase reveals the role of the saposin domain in activating substrate hydrolysis. *J. Mol. Biol.* **428**, 3026–3042 (2016).
30. J. Y. Lee *et al.*, Neuronal SphK1 acetylates COX2 and contributes to pathogenesis in a model of Alzheimer's disease. *Nat. Commun.* **9**, 1479 (2018).
31. J. Y. Lee *et al.*, N-AS-triggered SPMs are direct regulators of microglia in a model of Alzheimer's disease. *Nat. Commun.* **11**, 2358 (2020).
32. S. Zhu *et al.*, The role of neuroinflammation and amyloid in cognitive impairment in an APP/PS1 transgenic mouse model of Alzheimer's disease. *CNS Neurosci. Ther.* **23**, 310–320 (2017).
33. Q. Zeng, M. Zheng, T. Zhang, G. He, Hippocampal neurogenesis in the APP/PS1/nestin-GFP triple transgenic mouse model of Alzheimer's disease. *Neuroscience* **314**, 64–74 (2016).
34. D. C. Rubinsztein *et al.*, In search of an "autophagomometer." *Autophagy* **5**, 585–589 (2009).
35. C. Settembre *et al.*, TFEB links autophagy to lysosomal biogenesis. *Science* **332**, 1429–1433 (2011).
36. K. Biber, H. Neumann, K. Inoue, H. W. Boddeke, Neuronal 'on' and 'off' signals control microglia. *Trends Neurosci.* **30**, 596–602 (2007).
37. M. H. Park *et al.*, Characterization of the subventricular-thalamo-cortical circuit in the NP-C mouse brain, and new insights regarding treatment. *Mol. Ther.* **27**, 1507–1526 (2019).
38. A. Ghosh *et al.*, Alzheimer's disease-related dysregulation of mRNA translation causes key pathological features with ageing. *Transl. Psychiatry* **10**, 192 (2020).
39. K. Hernández-Ortega, P. Garcia-Esparcia, L. Gil, J. J. Lucas, I. Ferrer, Altered machinery of protein synthesis in Alzheimer's: From the nucleolus to the ribosome. *Brain Pathol.* **26**, 593–605 (2016).
40. S. Banerjee, S. Ferdosh, A. N. Ghosh, C. Barat, Tau protein-induced sequestration of the eukaryotic ribosome: Implications in neurodegenerative disease. *Sci. Rep.* **10**, 5225 (2020).
41. H. Boutej *et al.*, Diverging mRNA and protein networks in activated microglia reveal SRSF3 suppresses translation of highly upregulated innate immune transcripts. *Cell Rep.* **21**, 3220–3233 (2017).
42. Y. Yang *et al.*, Inflammation leads to distinct populations of extracellular vesicles from microglia. *J. Neuroinflammation* **15**, 168 (2018).
43. A. Tréfier *et al.*, G protein-coupled receptors as regulators of localized translation: The forgotten pathway? *Front. Endocrinol. (Lausanne)* **9**, 17 (2018).
44. J. L. Freeman *et al.*, Beta 2-adrenergic receptor stimulated, G protein-coupled receptor kinase 2 mediated, phosphorylation of ribosomal protein P2. *Biochemistry* **41**, 12850–12857 (2002).
45. B. K. Mani *et al.*, Neuroanatomical characterization of a growth hormone secretagogue receptor-green fluorescent protein reporter mouse. *J. Comp. Neurol.* **522**, 3644–3666 (2014).
46. B. K. Mani *et al.*, The role of ghrelin-responsive mediobasal hypothalamic neurons in mediating feeding responses to fasting. *Mol. Metab.* **6**, 882–896 (2017).
47. J. Tian *et al.*, Disrupted hippocampal growth hormone secretagogue receptor 1α interaction with dopamine receptor D1 plays a role in Alzheimer's disease. *Sci. Transl. Med.* **11**, eaav6278 (2019).
48. S. Tonegawa, M. D. Morrissey, T. Kitamura, The role of engram cells in the systems consolidation of memory. *Nat. Rev. Neurosci.* **19**, 485–498 (2018).
49. X. Cao *et al.*, Increased serum acylated ghrelin levels in patients with mild cognitive impairment. *J. Alzheimers Dis.* **61**, 545–552 (2018).
50. K. Majchrzak, K. Szyszko, K. M. Pawłowski, T. Motyl, M. Król, A role of ghrelin in cancerogenesis. *Pol. J. Vet. Sci.* **15**, 189–197 (2012).
51. B. K. Mani, J. M. Zigman, Ghrelin as survival hormone. *Trends Endocrinol. Metab.* **28**, 843–854 (2017).
52. G. Ferré *et al.*, Structure and dynamics of G protein-coupled receptor-bound ghrelin reveal the critical role of the octanoyl chain. *Proc. Natl. Acad. Sci. U.S.A.* **116**, 17525–17530 (2019).
53. B. J. Bender *et al.*, Structural model of ghrelin bound to its G protein-coupled receptor. *Structure* **27**, 537–544.e4 (2019).
54. L. Y. Ma *et al.*, Ghrelin-attenuated cognitive dysfunction in streptozotocin-induced diabetic rats. *Alzheimer Dis. Assoc. Disord.* **25**, 352–363 (2011).
55. Y. Fisher, A. Nemirovsky, R. Baron, A. Monsonego, Dendritic cells regulate amyloid-β-specific T-cell entry into the brain: The role of perivascular amyloid-β. *J. Alzheimers Dis.* **27**, 99–111 (2011).
56. K. M. Anderson *et al.*, Dual destructive and protective roles of adaptive immunity in neurodegenerative disorders. *Transl. Neurodegener.* **3**, 25 (2014).